Letter of Intent

Measurement of polarization observables in η-photoproduction with CLAS

J. Ball, M. Dugger, E. Pasyuk*(Spokesperson), B. G. Ritchie
Arizona State University, Tempe, AZ 85287-1504,

R. A. Arndt, W. J. Briscoe, I. I. Strakovsky, S. Strauch, R. L. Workman
The George Washington University, Washington, DC 20052

H. Crannell, F. J. Klein, D. I. Sober
The Catholic University of America, Washington, DC 20064

C. Djalali, A. Dzyubak, D. Tedeschi, M. Wood
University of South Carolina, Columbia, SC 29208

D. Lawrence, R. Miskimen
University of Massachusetts, Amherst, MA 01003

P. L. Cole
University of Texas at El Paso, El Paso, TX 79968

D. Jenkins
Virginia Polytechnic Institute and State University, Blacksburg, VA 24061

L. Todor
Carnegie Mellon University, Pittsburgh, PA 15213

J. C. Sanabria
Universidad de los Andes, A.A. 4976, Santafé de Bogota, Colombia

M. F. Vineyard
Union College, Schenectady, NY 12308

*Contact person, E-mail:pasyuk@jlab.org

Abstract

We propose to measure with CLAS and the photon tagger in Hall B of Jefferson Lab the observables $d\sigma/d\Omega$, Σ, T, P, E, F, G, and H in η-photoproduction, using a polarized photon beam and polarized target. The measurements will span the range of W from 1.6 to 2.0 GeV with angular distributions spanning $\cos\theta_{\rm c.m.}$ from -0.9 to 0.9. The data obtained will provide information essential to understanding the nucleon resonance spectrum. The experiment requires the construction of a frozen spin target for use with CLAS.

Motivation

Among the most exciting and challenging topics in subnuclear physics today is the study of the structure of the nucleon and its different modes of excitation, the baryon resonances. Initially, most of the information on these excitations came primarily from partial wave analyses of data from πN scattering. Recently, these data have been supplemented by a large amount of information from pion electro- and photoproduction experiments. Yet, in spite of extensive studies spanning decades, many of the baryon resonances are still not well established and their parameters (i.e., mass, width, and couplings to various decay modes) are poorly known. Much of this is due to the complexity of the nucleon resonance spectrum, with many broad, overlapping resonances coupling to the πN channel.

While traditional theoretical approaches have highlighted a semi-empirical approach to understanding the process as proceeding through a multitude of s-channel resonances with a nonresonant background (as discussed in, for example, Ref. [1]), more recently attention has turned to approaches based on the underlying constituent quarks. An extensive review of the quark models of baryon masses and decays can be found in Ref. [2]. While these quark approaches are more fundamental and hold great promise, all of them predict many more resonances than have been observed, leading to the so-called "missing resonance" problem.

Additional progress in pinning down the details of the nucleon resonance spectrum can be made by looking at reaction channels and observables which select particular resonances from the spectrum. In this regard, photoproduction of η-mesons provides a valuable "isospin filter" for the baryon resonance spectrum. Because of the quantum numbers of the η-meson this process directly couples only to isospin $I = \frac{1}{2}$ resonances. This has led to significant activity in recent years on electro- and photoproduction of these mesons.

While these experiments have established that the $S_{11}(1535)$ resonance dominates the reaction near threshold, there are nonetheless many questions concerning its properties, such as why the $S_{11}(1535)$ couples to ηN channel so strongly while higher mass resonances couple so weakly. Furthermore, as more data have become available from η production, comparisons with properties determined from pion production results have revealed apparent discrepancies. Two such examples involve the helicity amplitudes for this resonance, which had been thought to be well established with the existing pion photoproduction data. As pointed out in the last edition of the Review of Particle Physics[3], fits to η photoproduction data have given $N\gamma$ amplitudes for $S_{11}(1535)$ that are substantially larger than those extracted from fits to π-production data. More recent analyses [4, 5] have considered the sensitivity of this reaction to contributions from the $D_{13}(1520)$. The ratio of $D_{13}(1520) \rightarrow N\gamma$ amplitudes $A_{3/2}/A_{1/2}$ was found to be $-2.5 \pm 0.5 \pm 0.4$ in[4] and -2.1 ± 0.2 in [5]. Results inferred from π photoproduction are about a factor of three larger in magnitude[6]. The η photoproduction result is particularly surprising, as the $D_{13}(1520)$ has a very clean resonance signature in π photoproduction. Thus, despite the dominance of the $S_{11}(1535)$ resonance near threshold, its relatively large cross section, and the growing database from η electro- and photoproduction experiments, our understanding of this resonance remains ambiguous, even though it is assigned a "4 star" status by the Particle Data Group.

Our knowledge for the coupling of higher mass N^* resonances to the ηN channel is much more limited. Table 1, taken from the Particle Data Group Review of Particle Physics, illustrates very well the current status of our knowledge of the N^* resonances: Only two of the 22 suggested N^* resonances have more than one "star" for the ηN channel, whereas 14 of those 22 resonances are known in the πN with three or four stars.

One of the obstacles in determining the couplings of the baryon resonances to $N\eta$ is that the coupling is generally very small. As a result, differential cross section data, though helpful, still pro-

Table 1. The status of the N and Δ resonances. Only those with an overall status of *** or **** are included in the main Baryon Summary Table.

			Status as seen in —						
Particle	$L_{2I\cdot 2J}$	Overall status	$N\pi$	$N\eta$	ΛK	ΣK	$\Delta\pi$	$N\rho$	$N\gamma$
$N(939)$	P_{11}	****							
$N(1440)$	P_{11}	****	****	*			***	*	***
$N(1520)$	D_{13}	****	****	*			****	****	****
$N(1535)$	S_{11}	****	****	****			*	**	***
$N(1650)$	S_{11}	****	****	*	***	**	***	**	***
$N(1675)$	D_{15}	****	****	*	*		****	*	****
$N(1680)$	F_{15}	****	****				****	****	****
$N(1700)$	D_{13}	***	***	*	**	*	**	*	**
$N(1710)$	P_{11}	***	***	**	**	*	**	*	***
$N(1720)$	P_{13}	****	****	*	**	*	*	**	**
$N(1900)$	P_{13}	**	**					*	
$N(1990)$	F_{17}	**	**	*	*	*			*
$N(2000)$	F_{15}	**	**	*	*	*	*	**	
$N(2080)$	D_{13}	**	**	*	*				*
$N(2090)$	S_{11}	*	*						
$N(2100)$	P_{11}	*	*	*					
$N(2190)$	G_{17}	****	****	*	*	*		*	*
$N(2200)$	D_{15}	**	**	*	*				
$N(2220)$	H_{19}	****	****	*					
$N(2250)$	G_{19}	****	****	*					
$N(2600)$	$I_{1\,11}$	***	***						
$N(2700)$	$K_{1\,13}$	**	**						

vide a very limited exploitation of this "isospin filter" tool. Despite these small couplings, however, these resonances should reveal themselves more clearly through the interference of amplitudes best isolated with polarization observables. The formalism and terminology for the various polarization observables of interest in η photoproduction are described in the Appendix.

To estimate the sensitivities of these different observables to the presence of different resonances, we have used predictions from the ETA-MAID[1] calculations. Figure 1 shows predictions for all observables from the polarized beam/polarized target (denoted BT in the Appendix) group. The calculations shown include the $S_{11}(1535)$, $S_{11}(1650)$, $P_{11}(1710)$, $P_{13}(1720)$, $D_{13}(1520)$, $D_{13}(1700)$, $D_{15}(1675)$, and $F_{15}(1680)$ resonances (full model calculation). Then, we "turned off" the $D_{15}(1675)$ resonance, resulting in the calculations shown in Fig. 2. To see the resulting changes more clearly, Fig. 3 illustrates the difference in the two calculations. The differential cross section differences are rather small, but one can see that, despite the rather small coupling (~ 0.001) to the $N\eta$ channel, the effect on polarization observables can be very large, up to 0.5.

Admittedly, this comparison has some limitations, but qualitatively this simple difference gives an idea about the sensitivity with which polarization observables permit the process to be probed. While the calculation was not refit to the data with this resonance turned off, the very small differences in the differential cross section indicate those data alone cannot provide a test as stringent as the polarization observables.

Figure 4 shows the coverage in photon energy, E_γ, and scattering angle, $\theta_{\rm c.m.}$, of the available experimental data on η photoproduction. The left-hand panel contains points indicating where differential and total cross sections exist. The database is dominated by three experiments: data from TAPS[7] near threshold (green triangles), data from GRAAL[8] (blue squares) and our new data from CLAS[9] (red circles), which will be discussed later. The right-hand panel similarly shows available polarization data, dominated by two data sets: beam asymmetry, Σ, measurements from GRAAL[10] (blue squares) and target asymmetry, T, measurements from ELSA[11] (green diamonds). Besides these five experiments that contribute the majority of the data, there are

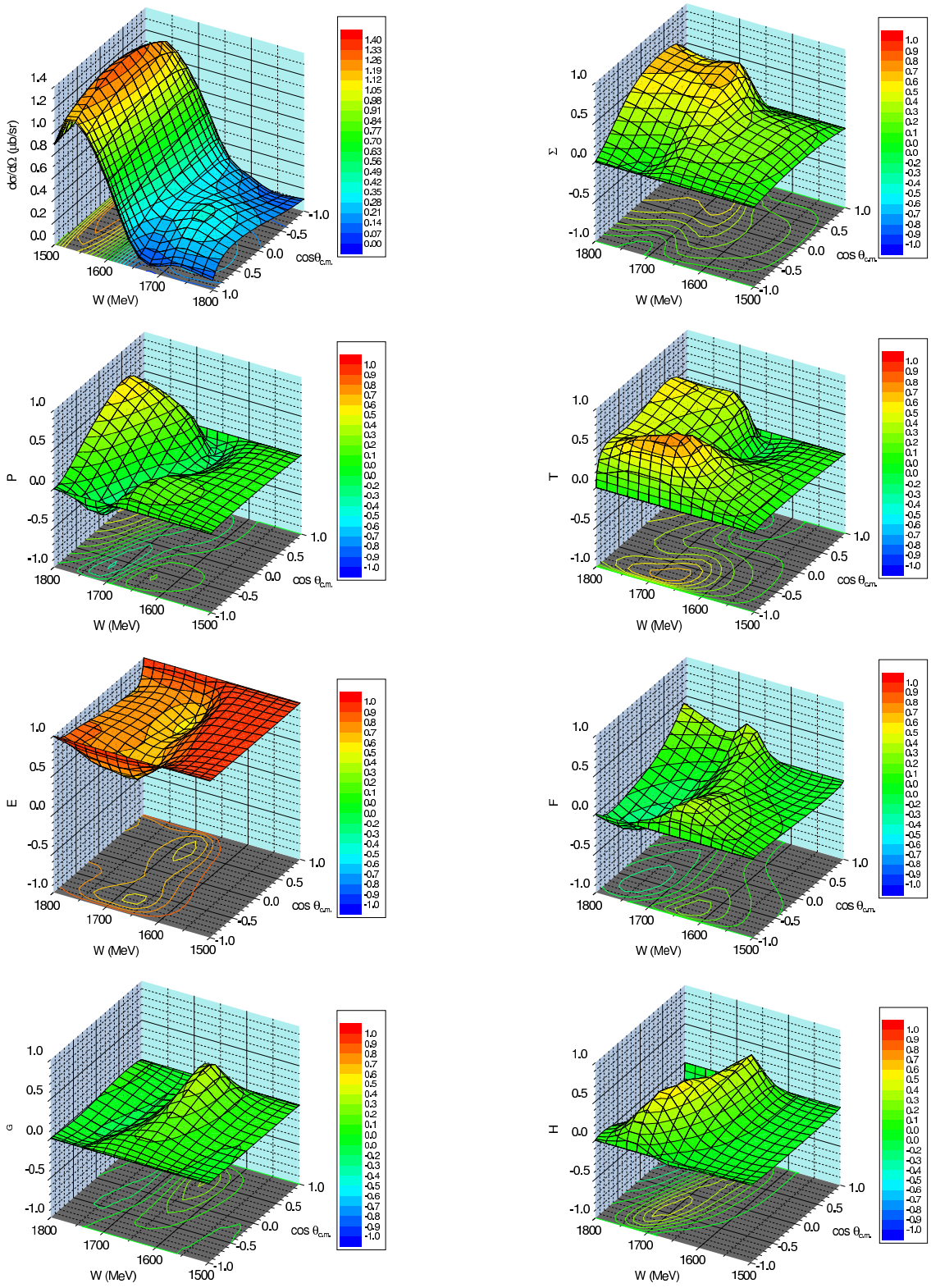

Figure 1: Predictions of ETA-MAID[1] for all polarization observables from the polarized photon beam/polarized target group of experiments.

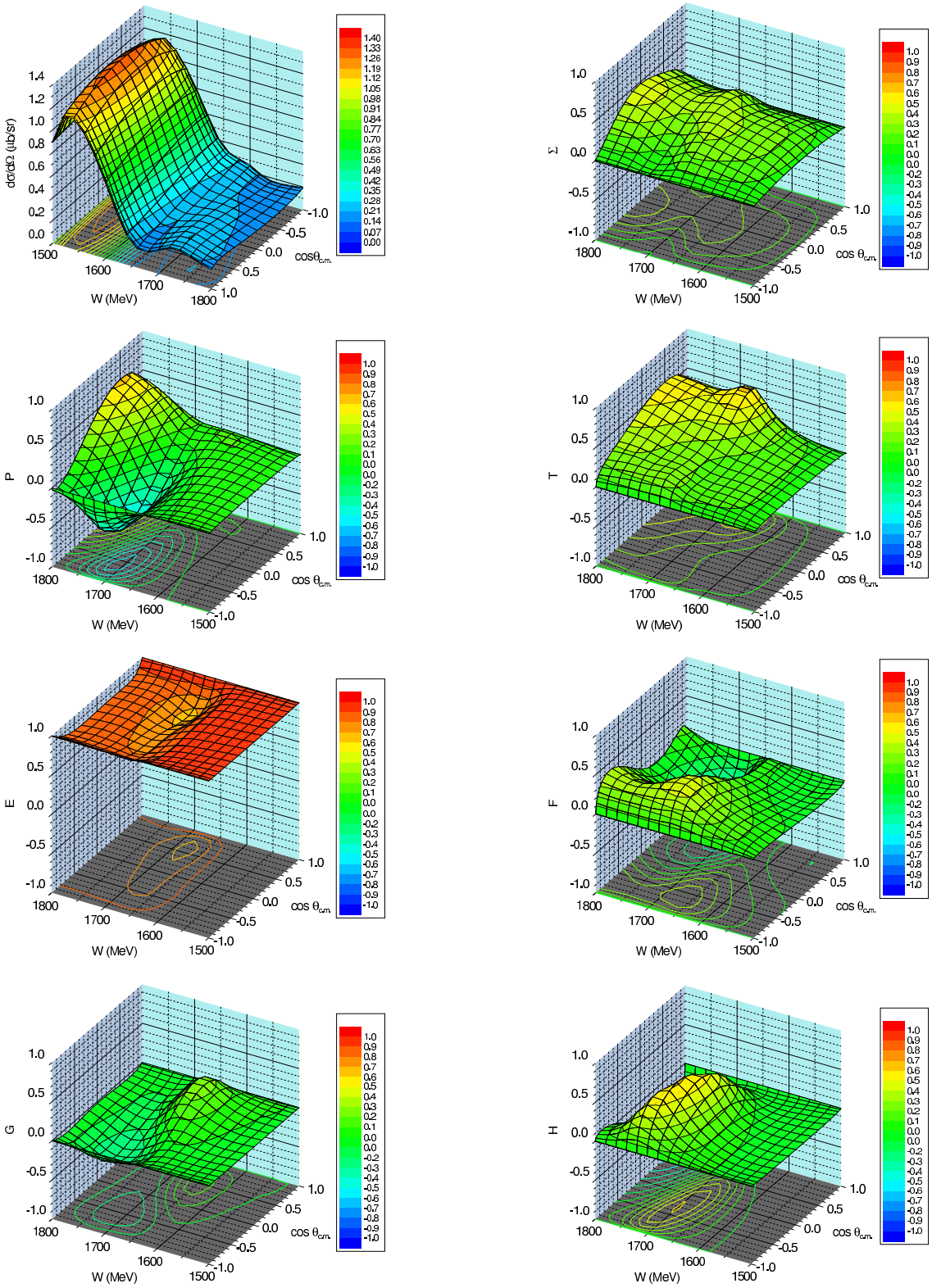

Figure 2: Same as Fig. 1 without the $D_{15}(1675)$ nucleon resonance.

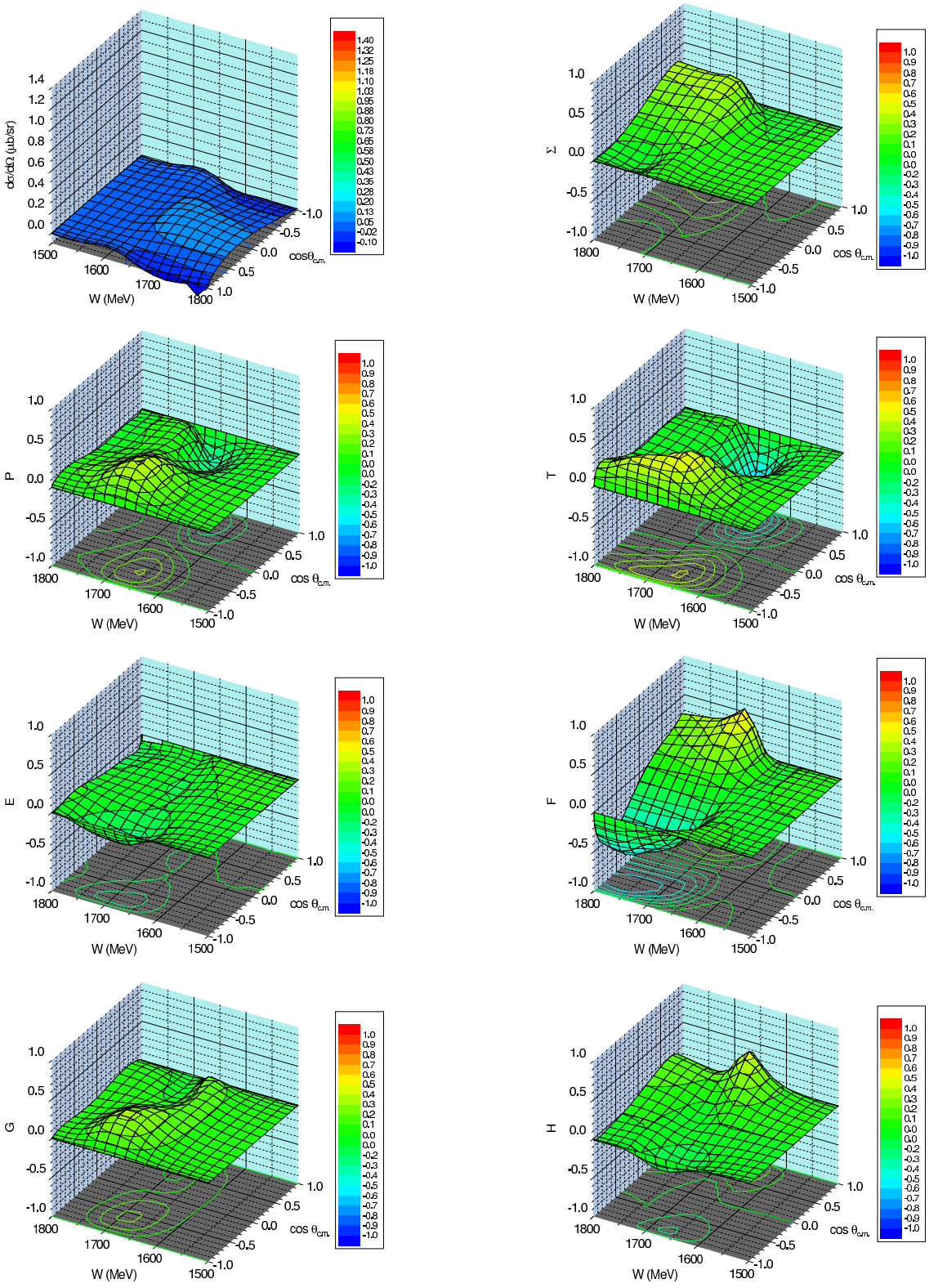

Figure 3: Difference between Figs. 1 and 2.

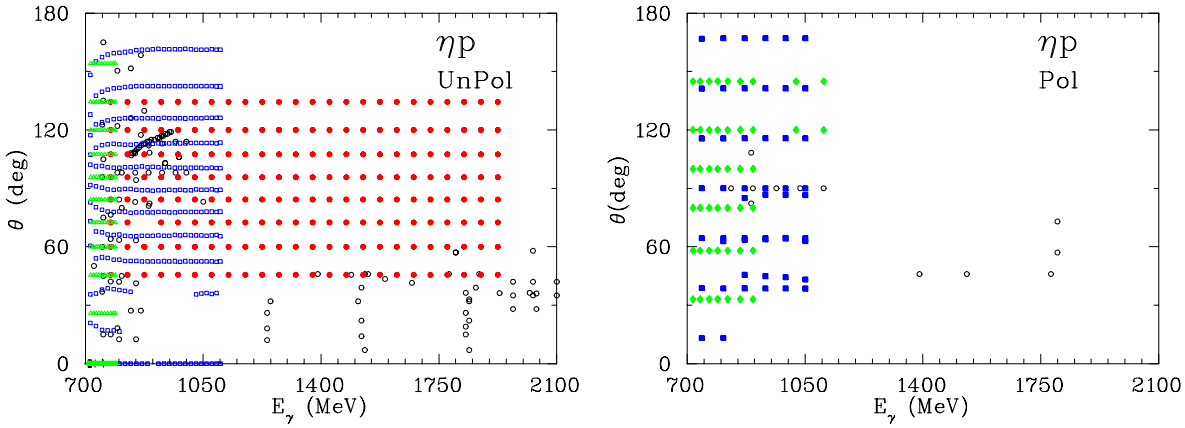

Figure 4: World database for η photoproduction.

several other experiments. Their data are shown by black circles. One can see that the coverage for cross sections in photon energy and scattering angle is now rather good from threshold and up to 2 GeV, with the exception of the most forward and most backward angles. On the other hand, polarization observables have been mainly measured in the region of $S_{11}(1535)$ resonance. Above that resonance exists a "desert" where models have considerable ambiguity, since many combinations of resonances can account for the available cross section data. Consequently, it is not surprising that we know little about the coupling of resonances above $W = 1.6$ GeV to $N\eta$. *With cross sections alone, there simply is insufficient information to constrain models in order to extract resonance parameters.*

Using CLAS and the photon tagger, we have, as noted above, provided new data on the differential cross sections for the reaction $\gamma p \to \eta p$ [9]. These new data illustrate the limitations of cross sections alone. The measured differential cross sections are presented in Fig. 5. In general, agreement between the new CLAS data and previous experiments is very good. This new data set extends to the previously unmeasured range of W from 1.7 to 2.1 GeV.

Figure 6 shows a comparison of the estimated total cross section with new predictions from both ETA-MAID[1] (REM) and from the chiral quark model of Saghai and Li[12] (χQM). The preliminary results of this new ETA-MAID fit generally reproduce the shapes of the observed cross sections quite well, including the forward peak seen at the highest energies, usually interpreted to be due to t-channel processes. However, while the REM shapes mimic what we observed, those calculations fall below our differential cross sections around W=1.85 GeV, and are somewhat above our data at $W \geq$1.9 GeV. With respect to the new χQM predictions, those calculations are generally in very good agreement with our data for $W \leq 1.9$ GeV. The inclusion of a third S_{11} resonance not predicted by the $SU(6)\otimes O(3)$ quark model in these preliminary calculations, with a mass 1.79 GeV and width of 250-350 MeV, markedly improved the fit to our data[12]. The agreement between our data and the χQM around W=1.85 GeV is considerably better than with the REM results. However, above W=1.9 GeV, the χQM approach begins to fall below our data, and the shapes predicted are inconsistent with the peak at forward angles in the differential cross section as the energy increases. This disagreement suggests additional resonances beyond those included in the χQM approach may be needed, and t-channel contributions not incorporated directly in that model may also be important.

These new cross sections certainly have provided some insight and direction into the these two theoretical approaches. Both approaches show regions of greater and lesser success, and the choice of which resonances are included in the ETA-MAID approach is particularly poorly constrained. It

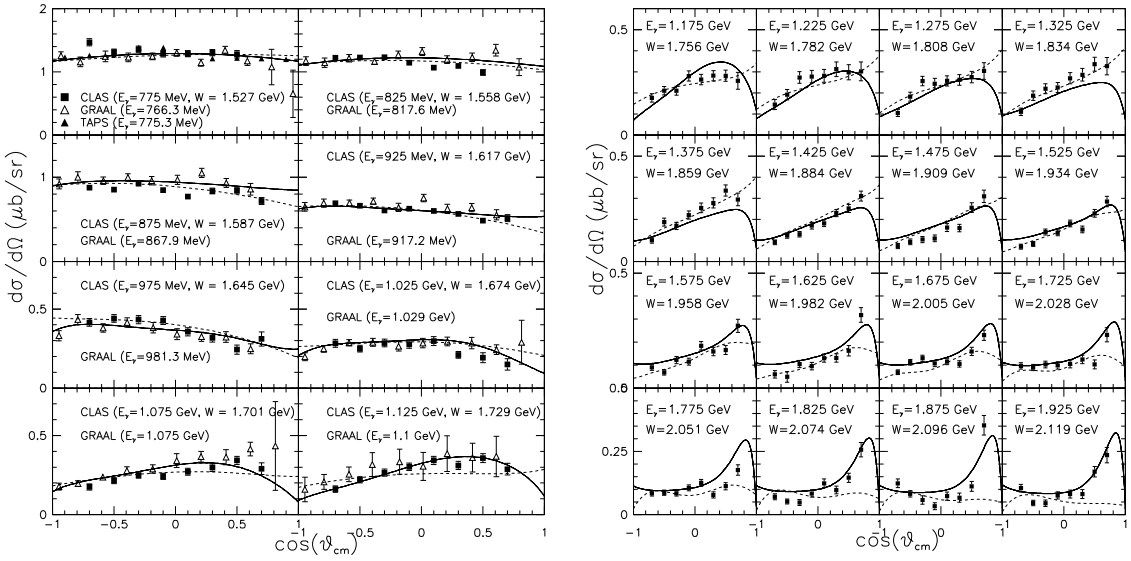

Figure 5: Differential cross section for $\gamma p \to p\eta$ measured with CLAS. Other results from TAPS[7] and GRAAL[8] are shown for comparison. Also shown are prediction from Refs. [1] (solid line) and [12] (dashed line).

is worth reiterating that, as seen above, while the models are more or less successful in reproducing the measured differential cross sections, they will be much more stringently tested with, for instance, target asymmetries. *Polarization observables are essential for making more progress.*

Overall, there are 16 different polarization observables for real photon experiments, and there are four independent helicity amplitudes. While several papers have been devoted to discussing a so-called "complete experiment"[13, 14, 15], there is no simple universal recipe on which, and how many, observables need to be measured for an unambiguous amplitude reconstruction. In general, if the unpolarized cross section and single spin observables Σ, P and T are measured one can reconstruct moduli of all four complex helicity amplitudes. However, their relative phases could not be unambiguously reconstructed. While single polarization observables are sensitive to the moduli of amplitudes, double polarization observables reflect their interference and thus could be used as a tool to measure their relative phases. As was shown in Ref. [14] in addition to unpolarized cross sections and single spin polarizations Σ, P and T, one needs **at least** four double spin observables. It was also shown that if all four are from the same group (either BT, BR or TR, as defined in the Appendix), ambiguities cannot be resolved. While the idea of a "complete experiment" and direct amplitude reconstruction sounds very attractive, accomplishing this goal is quite difficult: one needs to measure at least eight observables at each energy.

One method of extracting information from such data in a less model-dependent fashion than, say, the ETA-MAID or χQM approaches, is the partial wave analysis epitomized by the SAID facility[6, 16]. Originally these analyses were developed for NN and πN processes, but they have now been extended to meson (π, η, K) electro- and photoproduction data. In this approach, each of the helicity amplitudes is expressed in terms of multipoles. Multipoles, in turn, are functions of photon energy with a few adjustable parameters. These parameters are determined from the best fit to all available experimental data with some additional theoretical constraints. This approach allows the incorporation into one data set all available observables from different experiments at different energies and angles and account for their systematic uncertainties by means of adjustable

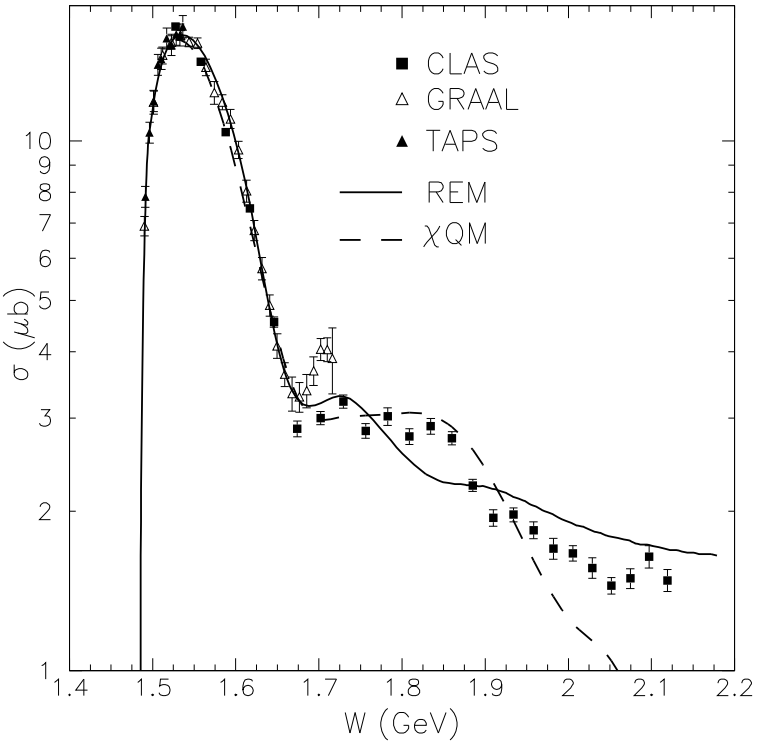

Figure 6: Total cross section estimates. Results from TAPS[7] and GRAAL[8] are shown for comparison. Curves are as in Fig. 5.

normalization factor specific for each experiment. Which multipoles must be included is not known a priori. It depends on the experimental data. *Polarization data are crucial for this procedure, however, since without them, the solution is poorly constrained.*

Proposed experimental program

Hall B provides a unique pair of instruments for these experiments: a large acceptance spectrometer which allows detection of particles in a wide range of θ and ϕ, and a unique broad-range photon tagging facility. Unpolarized, circularly-polarized and linearly-polarized tagged photon beams are presently available:

- For *unpolarized photon beams*, the Hall B photon tagger provides a range in photon energies from 20 to 95% of the incident electron beam energy. Most of the data taken thus far with real photons in Hall B has used this setup, and this mode of operation is well understood.
- With a polarized electron beam incident on the bremsstrahlung radiator, a circularly-polarized photon beam can be produced. For the photon energy range from 50 to 95% of the incident electron beam energy, the degree of circular polarization of the photon beam varies from 60 to 99% of the incident electron beam polarization.
- A linearly-polarized photon beam is produced by the coherent bremsstrahlung technique,

using an oriented diamond crystal as a radiator. This technique was successfully used during the CLAS-g8a running period. The degree of linear polarization depends on the fractional photon beam energy and collimation, and can be as high as 90%.

What is missing in Hall B for this experiment, however, is a polarized target for CLAS. With a frozen spin target for CLAS, the possibility will exist to have both transverse and longitudinal polarization. With such a target, we will be able to measure all single spin and all double spin observables from the beam/target group, for a total of eight observables: $d\sigma/d\Omega$, Σ, T, P, E, F, G, and H. (The other two groups of experiments (BR and TR) are not feasible with CLAS because it is not possible to put recoil polarimeter inside CLAS.)

[We note in passing that, using existing data sets, we already have CLAS data for the observables $d\sigma/d\Omega$ and Σ. The analysis of the first real photon beam run (CLAS-g1a) with an unpolarized photon beam has been completed[9]. The subsequent, much larger (20 times more) real photon run data set (CLAS-g1c) is being analyzed now. The first data with a linearly polarized beam (CLAS-g8a) have also already been taken and are under analysis.]

The proposed experimental program will consist of five experiments with different combinations of beam and target polarization:

1. Unpolarized beam – transversely-polarized target: Measurements of T;
2. Linearly-polarized beam – transversely-polarized target: Measurements of H and P;
3. Linearly-polarized beam – longitudinally-polarized target: Measurements of G;
4. Circularly-polarized beam – transversely-polarized target: Measurements of F;
5. Circularly-polarized beam – longitudinally-polarized target: Measurements of E.

Even though the recoil polarimeter is not available, P could be measured with linearly-polarized beam and transversely-polarized target in configuration when polarization vectors are parallel/anti-parallel.

Once all these observables are measured, Equations (1), (4), and (5), given in Appendix, could be used for consistency check and evaluation of systematic uncertainties.

We will detect the recoil proton in CLAS and use the missing mass technique to identify η photoproduction events, the same method as we used to obtain the data shown in Figs. 5 and 6[9]. The effects on recoil proton momentum determination of straggling in the target material and multiple Coulomb scattering in detector elements limit the angular coverage to $\cos\theta_{\rm c.m.}$ range from -0.9 to 0.9. However, this angular range is more than sufficient to provide very stringent tests on any current existing model or approach.

There are two main sources of background (and hence systematic uncertainties) associated with this technique:

- multipion production
- production on bound nucleons in polarized target (dilution factor).

In order to gain control of the first background, we will select other event topologies: In addition to recoil proton detection, we will require detection of η decay products. As for the dilution factor, we will put an auxiliary carbon target downstream of the polarized target and measure yield from the bound nucleons simultaneously.

Summary

We propose to measure with CLAS and the photon tagger in Hall B of Jefferson Lab the observables $d\sigma/d\Omega$, Σ, T, P, E, F, G, and H in η photoproduction with a polarized photon beam and polarized frozen spin target for W from 1.6 to 2.0 GeV, with $\cos\theta_{\rm c.m.}$ range from -0.9 to 0.9. These data will provide stringent tests of models of the nucleon, and provide a definitive data set for the nucleon resonance spectrum. The proposed experimental program is a natural continuation of research started in CLAS experiments E91-008[18] and E94-008[19], which measured η photoproduction on the proton and deuteron.

The experimental configuration partially overlaps the approved experiment E01-104[20] (Helicity structure of pion photoproduction). Some of the data could be taken simultaneously for those two experiments. There are a few other experiments on the photoproduction of other mesons ($\pi, K, \eta', \rho, \omega$, etc.) that are being proposed or expected to be proposed in the near future. All intend to use a frozen spin polarized target. The experimental conditions for these experiments are similar, which may allow most of the data to be taken simultaneously.

The preparation of the full proposal and experiment itself will require extensive simulation in order to determine optimal experimental conditions (electron beam energy, CLAS magnetic field, target dimensions and position), acceptance and detection efficiency, and to estimate the expected uncertainties and the required beam time. If the PAC finds this proposed experimental program interesting, we believe a full proposal could be prepared by the next PAC meeting.

This polarized target, if built, would be an invaluable tool for new generation of real photon experiments with CLAS, providing a combination of tools unique in the world.

Acknowledgment

The Arizona State University group is supported by the U. S. National Science Foundation.

Appendix

The definitions of the variables commonly used to describe meson photoproduction experiments could be found in Refs. [13, 17]. In η photoproduction there could be three polarized objects: photon beam, target and recoil proton. Figure 7 shows the coordinate system we will be using. The frame $\{x, y, z\}$ is related to the target polarization, with the z-axis along the photon momentum $\vec{k}$, the y-axis perpendicular to scattering plane $\vec{y} = \vec{k} \times \vec{q}/\sin\theta$, and x-axis is defined as $\vec{x} = \vec{y} \times \vec{z}$. The frame $\{x', y', z'\}$ is related to the recoil proton polarization, with z'-axis along the η momentum $\vec{q}$, y'-axis is the same as y-axis, and x'-axis is defined as $\vec{x} = \vec{y'} \times \vec{z'}$

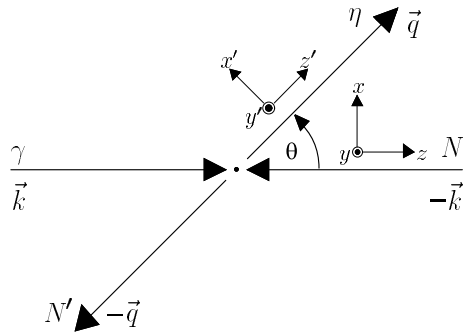

Figure 7: Coordinate systems for polarization vectors in η photoproduction in the c.m. system.

The differential cross sections may be determined by three groups of polarization experiments:

- polarized photons and polarized target (BT)

$$\begin{aligned}\frac{d\sigma}{d\Omega} &= \sigma_0\big[\,1 - P_T\,\Sigma\cos 2\varphi + P_x(-P_T H\sin 2\varphi + P_\odot F)\\ &\quad -P_y(-T + P_T P\cos 2\varphi) - P_z(-P_T G\sin 2\varphi + P_\odot E)\big]\,, \end{aligned} \tag{1}$$

- polarized photons and recoil polarization (BR)

$$\begin{aligned}\frac{d\sigma}{d\Omega} &= \sigma_0\big[\,1 - P_T\,\Sigma\cos 2\varphi + P_{x'}(-P_T O_{x'}\sin 2\varphi - P_\odot C_{x'})\\ &\quad -P_{y'}(-P + P_T T\cos 2\varphi) - P_{z'}(P_T O_{z'}\sin 2\varphi + P_\odot C_{z'})\big]\,, \end{aligned} \tag{2}$$

- polarized target and recoil polarization (TR)

$$\begin{aligned}\frac{d\sigma}{d\Omega} &= \sigma_0\big[\,1 + P_{y'}P + P_x(P_{x'}T_{x'} + P_{z'}T_{z'})\\ &\quad +P_y(T + P_{y'}\Sigma) - P_z\,(P_{x'}L_{x'} - P_{z'}L_{z'})\big]\,, \end{aligned} \tag{3}$$

where σ_0 denotes the unpolarized differential cross section, P_T the transverse degree of photon polarization, $P_\odot$ the right-handed circular photon polarization, φ the angle between photon polarization vector and reaction plane, and $\vec{P}$ the target polarization. Table 2 summarizes all polarization observables.

These 16 observables are not completely independent. Their relations could be used for the consistency check of the experimental data and for the evaluation of systematic uncertainties.

Table 2: Polarization observables in pseudoscalar meson photoproduction. The entries in parentheses signify that the same polarization observables also appear elsewhere in the table.

Beam	Target				Recoil			Target + Recoil			
	–	–	–	–	x'	y'	z'	x'	x'	z'	z'
	–	x	y	z	–	–	–	x	z	x	z
unpolarized	σ_0	0	T	0	0	P	0	$T_{x'}$	$-L_{x'}$	$T_{z'}$	$L_{z'}$
linear pol.	$-\Sigma$	H	$(-P)$	$-G$	$O_{x'}$	$(-T)$	$O_{z'}$	$(-L_{z'})$	$(T_{z'})$	$(-L_{x'})$	$(-T_{x'})$
circular pol.	0	F	0	$-E$	$-C_{x'}$	0	$-C_{z'}$	0	0	0	0

Since in this letter we discuss only the Beam-Target group we present relations only for these observables. There are two relations for this group:

$$E^2 + F^2 + G^2 + H^2 = 1 + P^2 - \Sigma^2 - T^2, \tag{4}$$

and

$$FG - EH = P - \Sigma T. \tag{5}$$

References

[1] W. -T. Chiang, S. -N. Yang, L. Tiator and D. Drechsel, Nucl. Phys. **A700**, 429 (2002); W. -T. Chiang, private communication.

[2] S. Capstick and W. Roberts, Prog. Part. Nucl. Phys. (Suppl. 2), **45**, S241 (2000).

[3] D. E Groom *et al.*, *Review of Particle Physics*, Eur. Phys. J. C **15** 1 (2000).

[4] N. C. Mukhopadhay and N. Mathur, Phys. Lett. **B444**, 7 (1998).

[5] L. Tiator, D. Drechsel, and G. Knöchlen, Phys. Rev. C **60**, 035210 (1999).

[6] R. A. Arndt, I. I. Strakovsky, and R. L. Workman, Phys. Rev. C **53**, 430 (1996).

[7] B. Krusche, *et al.*, Phys. Rev. Lett. **74**, 3736 (1995).

[8] F. Renard, *et al.*, Phys. Lett. B **528**, 215 (2002).

[9] M. Dugger and CLAS collaboration, under collaboration review.

[10] J. Ajaka *et al.*, Phys. Rev. Lett **81**, 1797 (1998).

[11] A. Bock *et al.*, Phys. Rev. Lett. **81**, 534 (1998).

[12] B. Saghai and Z. Li, Eprint: nucl-th/0202007; B. Saghai, private communication.

[13] I. S. Barker, A. Donnachie, and J. K. Storrow, Nucl. Phys. **B95**, 347 (1975).

[14] W.-T. Chiang and F. Tabakin, Phys. Rev. C **55**, 2054 (1997).

[15] G. Keaton and R. Workman, Phys. Rev. C **53**, 1435 (1996).

[16] R. A. Arndt, I. I. Strakovsky, and R. L. Workman, Phys. Rev. C **62**, 034005 (2000); R. A. Arndt, I. I. Strakovsky, R. L. Workman, and M. M. Pavan, Phys. Rev. C **52**, 2120 (1995); R. A. Arndt, I. I. Strakovsky, and R. L. Workman, in: *Proc. of 9th International Symposium on Meson-Nucleon Physics and the Structure of the Nucleon, Washington, DC, USA, July 26–31, 2001*, Eds. H. Haberzettl and W. J. Briscoe, πN Newslett. **16**, 150 (2002).

[17] C. G. Fasano, F. Tabakin and B. Saghai, Phys. Rev. C **46** 449 (1992).

[18] TJNAF experiment E91-008 (1991): "Photoproduction of η and η' mesons," Spokesperson: B. G. Ritchie.

[19] TJNAF experiment E94-008 (1994): "Photoproduction of η and η' mesons from deuterium," Spokesperson: B. G. Ritchie.

[20] TJNAF experiment E01-104 (2001): "Helicity structure of pion photoproduction," Update of experiment E91-005, Spokespersons: D. Crabb, M. Khandaker, D. I. Sober.